Tumor Targeting via Sialic Acid [^{68}Ga]DOTA-en-pba as a New Tool for Molecular Imaging of Cancer with PET

Tsoukalas, Charalambos; Geninatti-Crich, Simonetta; Gaitanis, Anastasios; Tsotakos, Theodoros; Paravatou-Petsotas, Maria; Aime, Silvio; Jiménez-Juárez, Rogelio; Anagnostopoulos, Constantinos D.; Djanashvili, Kristina; Bouziotis, Penelope

DOI
10.1007/s11307-018-1176-0

Publication date
2018

Document Version
Accepted author manuscript

Published in
Molecular Imaging and Biology

Tumor targeting via sialic acid: [^{68}Ga]-DOTA-en-pba as a new tool for molecular imaging of cancer with PET

Charalambos Tsoukalas[1], Simonetta Geninatti-Crich[2], Anastasios Gaitanis[3], Theodoros Tsotakos[1], Maria Paravatou-Petsotas[1], Silvio Aime[2], Rogelio Jiménez-Juárez[4,5], Constantinos D. Anagnostopoulos[3], Kristina Djanashvili[5], Penelope Bouziotis[1]

Shortened title as running head: PET Imaging of Tumors through Sialic Acid recognition

Manuscript Category: Original Article

[1]Institute of Nuclear & Radiological Sciences & Technology, Energy & Safety, National Center for Scientific Research "Demokritos", Aghia Paraskevi 15310, Athens, Greece
[2]University of Turin, Department of Molecular Biotechnology and Health Sciences, via Nizza 52, Torino, Italy
[3]Biomedical Research Foundation of the Academy of Athens, 4 Soranou Ephessiou Street, 11527, Athens, Greece
[4]Department of Organic Chemistry, National School of Biological Sciences, National Polytechnical Institute, Prolongación de Carpio y Plan de Ayala S/N, 11340 Mexico D.F., Mexico
[5]Department of Biotechnology, Delft University of Technology, Van der Maasweg 2629 HZ, Delft, Netherlands

**Corresponding author: Dr. Penelope Bouziotis, E-mail: bouzioti@rrp.demokritos.gr;*

Phone: +30 210 6503687, 0030 6973348788; Fax: +30 210 6545496

Abstract

Purpose: The aim of this study was to demonstrate the potential of gallium-68 labeled macrocycle (DOTA-en-pba) conjugated with phenylboronic vector for tumor recognition by PET, based on targeting of the overexpressed sialic acid (Sia).

Procedures: The imaging reporter DOTA-en-pba was synthesized and labeled with gallium-68 at high efficiency. Cell binding assay on Mel-C and B16-F10 melanoma cells was used to evaluate melanin production and Sia overexpression to determine the best model for demonstration the capability of [^{68}Ga]-DOTA-en-pba to recognize tumors. The *in vivo* PET imaging was done with B16-F10 tumor-bearing SCID mice injected with [^{68}Ga]-DOTA-en-pba intravenously. Tumor, blood, and urine metabolites were assessed to evaluate the presence of targeting agent.

Results: The affinity of [^{68}Ga]-DOTA-en-pba to Sia was demonstrated on B16-F10 melanoma cells, after the production of melanin as well as Sia overexpression was proved to be up to 4 times higher in this cell line compared to Mel-C cells. Biodistribution studies in B16-F10 tumor-bearing SCID mice showed blood clearance at the time points studied, while uptake in the tumor peaked at 60 min p.i. (6.36 ± 2.41 % ID/g). The acquired PET images were in accordance with the *ex vivo* biodistribution results. Metabolite assessment on tumor, blood and urine samples showed that [^{68}Ga]-DOTA-en-pba remains unmetabolized up to at least 60 min post-injection.

Conclusions: Our work is the first attempt for *in vivo* imaging of cancer by targeting overexpression of sialic acid on cancer cells with a radiotracer in PET.

Key words: Sialic acid, Tumor recognition, Phenylboronic targeting vector, Gallium-68, PET imaging

Introduction

Cancer diagnosis has significantly been improved over the past decades, due to novel imaging agents that enable earlier detection. Recently, the development of tailored therapies to perform personalized treatment of cancer is under intense scrutiny. These new personalized medicine approaches require, together with the finding of new tumor biomarkers, the development of fast, sensitive, and quantitative methods for the measurements of clinically relevant markers in order to propose the best treatment for each patient [1-2]. One of the most characteristic examples of a successful tumor imaging agent is the diagnostic peptide [^{111}In-DTPA]octreotide, which has been used for over 20 years to localize somatostatin receptors overexpressed in neuroendocrine tumors (NETs). In recent years, the theranostic approach has gained popularity, where disease staging and therapy are performed with the same biomolecule radiolabeled with either a diagnostic or a therapeutic isotope. These diagnostic/therapeutic probes, otherwise known as theranostic probes, are key players in simultaneous disease detection, treatment and consequent treatment assessment [3-5].

Sialylation is an important modification in cellular glycosylation. In fact, sialylated carbohydrates have a fundamental role in cellular signaling, adhesion and recognition [6]. An increase in total sialylation has been closely associated with cancer and the overexpression of polysialic acid frequently occurs in high-grade tumors and metastasis [7]. For example, polysialic acid can often be present in neural cell adhesion molecule 1 (NCAM1), and this is associated with aggressiveness and poor clinical outcome in lung cancer, neuroblastoma and gliomas [8-9]. Moreover, gangliosides (glycosphingolipid containing one or more sialic acids) are overexpressed in melanoma, neuroblastoma and breast cancer in which they mediate cell proliferation, tumor growth, and cancer cell migration [10]. Since sialylation plays a fundamental role in the dissemination of cancer cells from primary tumors, the development of new treatments able to interfere with sialic acid (Sia) overexpression in cancer cells may

provide a means of preventing cancer metastasis [11]. To this purpose many strategies have been proposed: i) desialylation of cancer cells by overexpressing human sialidases [12]; ii) treatment with bacterial sialidases [13]; iii) synthetic small molecules that inhibit Sia expression [11]. The key success of these personalized therapies is strictly dependent on the availability of non-invasive imaging methods able to report on Sia overexpression on the tumor cell surface before and after treatment. Currently, the determination of the sialylation status of solid tumors is carried out on biopsies or indirectly on patient serum. The first procedure is semi-quantitative and strongly dependent on sampling and the use of an unrepresentative tissue sample for the whole, potentially heterogeneous tumor may cause the occurrence of false-positive or false-negative evaluations. Subsequently, probes that can non-invasively visualize Sia *in vivo* on the tumor cell surface present particular research interest.

The synthesis of a magnetic resonance imaging (MRI) contrast agent (CA) DOTA-en-pba capable of targeting Sia residues has been recently reported [14]. The targeting moiety in this MRI CA is phenylboronic acid (pba) that can selectively form five- and six-membered cyclic boronate esters with the exocyclic polyol function of Sia. DOTA (1,4,7,10-tetraazacyclododecane-1,4,7,10-tetraacetic acid), conjugated to the pba targeting vector through an ethylenediamine (en) spacer, served as a chelate for stable complexation with the paramagnetic Gd^{III}. MRI as an imaging technique is characterized by high temporal and spatial resolution [15]. However, molecular MRI requires high concentrations of the imaging probe and prescans to determine the background level of MRI signal prior to CA administration [16]. In contrast, in radionuclide molecular imaging, such as positron emission tomography (PET), prescans are not needed. Also due to its advantages of high sensitivity, limitless penetration depth and quantitative capabilities, PET offers the potential to detect diseases alterations at molecular and cellular level [17].

Among available PET radionuclides, one of the most attractive for medical applications is gallium-68 due to its favorable physical characteristics [18-20]. Gallium-68 decays at 89% through positron emission of 1.92 MeV (maximum energy) and can be eluted from an in-house $^{68}Ge/^{68}Ga$ generator (^{68}Ge, $T_{1/2}$ = 270.8 days), thus providing an ideal positron-emitting isotope without the need for an on-site cyclotron. Furthermore, its physical half-life of 68 min renders it compatible with the *in vivo* pharmacokinetics of many peptides and antibody fragments [19-20]. One of its main advantages is that it can be used as the diagnostic analogue of many trivalent radionuclides, for which the coordination chemistry is fully developed. In other words, the same chelator can be used for efficient labeling with the diagnostic radionuclide gallium-68 and with other therapeutic nuclides such as yttrium-90 and lutetium-177 [21]. In this work, we exploit the versatility of DOTA-en-pba targeting agent and demonstrate its potential to be applied as a radiotracer for positron emission tomography (PET) imaging of cancer after labeling with radioactive gallium-68.

Materials and Methods

General

All reagents and solvents were of chemical grade and used without further purification. DOTA-en-pba was synthesized according to the previously reported procedure [14]. High Performance Liquid Chromatography (HPLC) was performed using a Waters 600 Controller pump, a Waters 996 Photodiode Array detector and a γ-RAM Radioactivity detector to measure radioactive flow. The UV detection wavelength was 295 nm for all experiments. A lower activity commercial $^{68}Ge/^{68}Ga$ generator was acquired from Eckert & Ziegler (Berlin, Germany). HPLC analyses were performed on a Waters μ-Bondapack C18 (3.9 mm i.d. × 300 mm) cartridge column (Waters, Germany). The gradient systems used are mentioned in the text.

HPLC solvents of analytical grade were filtered through 0.22 μm membrane filters (Millipore, Milford, MA) and degassed before use. Radioactivity measurements were conducted in an automated well-typed γ-counter NaI(Tl) crystal (Packard). Tissue and blood samples were measured on a Packard COBRA II Auto-Gamma counter (Canberra, USA). The mouse melanoma cell line B16-F10 was acquired from the American Type Culture Corporation. The human melanoma cell Mel-C line was donated by the Biology Department of the National Kapodistrian University of Athens. For cell culturing, Dulbecco's modified Eagle medium (DMEM), fetal bovine serum (FBS), penicillin/streptomycin, L-glutamine, and trypsin/EDTA solution were purchased from PAA Laboratories (GmbH, Austria). The bovine serum albumin (BSA), glutamax, HEPES, bacitracin, aprotinin, and PMSF used were obtained from Sigma-Aldrich (GmbH, Austria). Animals used for the biodistribution studies were obtained from the breeding facilities of the Institute of Biological Sciences, National Center for Scientific Research, Demokritos, Athens, Greece.

Radiolabeling of DOTA-en-pba with gallium-68

Gallium-68 was eluted from the $^{68}Ge/^{68}Ga$ generator with 7 mL 0.1 N HCl and trapped onto an acidic cation-exchange resin. Metal impurities (such as Zn, Fe, Ti and Ge) were removed by passage of 1 mL of washing solution containing acetone (80 v/v%) and 0.15 M HCl (20v/v%) [22]. Subsequent desorption of purified gallium-68 from the cation-exchanger was afforded with 400 μL of acetone (97.6 v/v%) and 0.15 M HCl (2.4 v/v%). For a typical preparation of gallium-68 labeled DOTA-en-pba, 50 μL (1 mg/mL stock solution, 50 μg/86.2 nmol) of DOTA-en-pba dissolved in ultrapure H_2O was mixed with sodium acetate buffer (pH 3.6) and 200 μL of gallium-68 eluate (~80 MBq) were consequently added. The mixture was then incubated for 30 min at 90 °C. Radiochemical purity was determined by HPLC, using a gradient system for elution. For the quality control of radiolabeling, 10 μL aliquots of the

reaction solution were analyzed by RP-HPLC, applying a linear gradient system at a 1 mL/min flow rate from 0% B to 100% B in 20 min, where solvent A = 0.05% TFA in H_2O and solvent B = 0.05% TFA in AcCN. The radiolabeled complex was used without further purification.

In vitro stability of [^{68}Ga]-DOTA-en-pba

In vitro stability of [^{68}Ga]- DOTA-en-pba was assessed in saline and serum for up to 3h. For the labeling stability experiment in serum, [^{68}Ga]-DOTA-en-pba (~0.4 MBq/100 μL) was incubated with 900 μL human serum in a 37 °C water bath for 60, 120 and 180 min and then analyzed by ITLC-SG (mobile phase: 0.1 M Na_2CO_3, gallium-68 ions remained at the origin, while the labeled compound moved with the solvent front; mobile phase: 0.1 M HCl, gallium-68 ions moved with the solvent front, while the labeled compound remained at the origin). For stability assessment in saline, [^{68}Ga]-DOTA-en-pba (~0.4 MBq/100 μL) was incubated with 900 μL saline at room temperature, and samples were taken at 60, 120 and 180 min and then analyzed by ITLC-SG, as described above. All assays were performed in triplicate.

In vitro cell binding assay

In vitro cell binding experiments were performed on Human Mel-C and Mouse B16-F10 melanoma cells, in order to assess the targeting capability of [^{68}Ga]-DOTA-en-pba to the Sia-residues. Both B16-F10 and Mel-C cells were cultured in standard DMEM complete (10% FBS, 1% penicillin/streptomycin, 1% L-glutamine). Cells were incubated at 37 °C in a humidified atmosphere of 5% CO_2. On day prior to experiments, B16-F10 and Mel-C cells were seeded in 24-well plates and grown to confluency. For the binding experiment, 0.5 nmol of [^{68}Ga]-DOTA-en-pba were added to each well and incubated for 1h at 37 °C. Subsequently, the supernatant was removed, the cells were washed 3 times with ice-cold PBS and lysed by the addition of 1M NaOH. Activity was measured, along with an aliquot with the initial

activity, representing 100% added activity. The percent cell uptake was then calculated. Non-specific binding was determined in parallel, in the presence of 25 nmol of unlabeled DOTA-en-pba, with 1h of pre-incubation.

Evaluation of melanin production and sialic acid expression

B16-F10 and Mel-C cells were grown in 6 cm diameter dishes. When the dishes reached 70-80% confluence, cells were detached with trypsin/EDTA, washed twice with 10 mL of PBS and collected in ca. 100-200 μL of PBS. Then, NaOH was added to the cells lysate to a final concentration of 0.1 M and final volume of 700 μL. The samples are heated for 1h at 60 °C. The melanogenesis was evaluated by measuring the absorbance at 490 nm. The protein content of cell lysates was measured by Bradford assay. Sia expression on B16-F10 and Mel-C cells was determined using a commercially available AbCAM assay (NANA assay Kit) on the same lysate sample.

Ex vivo biodistribution studies

All applicable institutional and/or national guidelines for the care and use of animals were followed. These studies have been further approved by the Ethics Committee of the NCSR "Demokritos" and animal care and procedures followed are in accordance with institutional guidelines and licenses issued by the Department of Agriculture and Veterinary Policies of the Prefecture of Attiki (Registration Numbers: EL 25 BIO 022 and EL 25 BIO 021). For experimental tumor models, female SCID mice of 8 weeks on the day of inoculation were obtained from the breeding facilities of the Institute of Biology, NCSR "Demokritos". Mel-C human melanoma cells and B16-F10 mouse melanoma cells (1×10^7 cells) were subcutaneously inoculated into two separate cohorts of mice. The animals, housed in air-conditioned rooms under a 12 h light/dark cycle, were allowed free access to food and water.

Approximately two weeks after inoculation, *ex vivo* biodistribution studies and *in vivo* imaging studies on the tumor-bearing mice were performed (tumor size at the initiation of experiments: ~ 0.5 cm^3).

[^{68}Ga]-DOTA-en-pba was intravenously administered via the tail vein. Each mouse received 2.0 ± 0.5 MBq/5.75 nmol/100 μL of the gallium-68 labeled imaging reporter. The biodistribution study was performed at 30, 60 and 120 min for both the Mel-C and B16-F10 tumor-bearing mice (n = 4 per time-point). At the times indicated, the mice were euthanized and the organs of interest, such as the heart, liver, kidneys, stomach, intestines, spleen, lungs, pancreas, bones, and tumor were removed, weighed and counted in a NaI well-counter (Packard COBRA II auto gamma counter) together with samples of muscles and urine. All measurements were corrected for background and radioactive decay. Tissue distribution data were calculated as the percent injected dose per gram (% ID/g), using an appropriate standard. Stomach and intestines were not emptied before the measurements. The % ID in whole blood was estimated assuming a whole-blood volume of 6.5% of the total body weight.

Binding specificity of [^{68}Ga]-DOTA-en-pba was assessed in B16-F10 melanoma tumor-bearing mice (n = 4 mice), after pre-injection of the mice with 0.2875 μmol/100 μL "cold" DOTA-en-pba. For reasons of direct comparison, a second cohort of B16-F10 tumor-bearing mice (n = 4 mice) received [^{68}Ga]-DOTA-en-pba (5.75 nmol/100 μL). Both groups of mice were euthanized at 60 min post-injection of the radiotracer.

Metabolite evaluations

In urine and plasma*:* Urine and blood metabolite assessment was performed at 15, 30 and 60 min p.i., in order to determine the metabolic rate of [^{68}Ga]-DOTA-en-pba after injection. Urine was collected at euthanizing time and centrifuged for 10 min at 2000 g before RP-HPLC

analysis. Blood collected from mice at the same time-points was also centrifuged for 10 min at 2000 g and the supernatant (serum) was collected. Serum was treated with twice the volume of cold EtOH for protein precipitation. The resulting serum sample was injected onto the RP-HPLC column for analysis.

In tumor*:* Tumor samples were rapidly cut into small pieces and added to ice-cold PBS. Samples were homogenized, the resulting homogenate was centrifuged for 15 min at 2000 g. The supernatant was filtered through a 0.2 μm membrane before HPLC analysis, and 200 μL of the filtrate was directly injected onto the HPLC column. The data processing was the same as described above for urine and serum.

PET imaging studies

To confirm the feasibility of using [^{68}Ga]-DOTA-en-pba to detect melanoma, *in vivo* micro-PET scans were performed on the B16-F10 tumor model. Three mice (n=3) were fasted prior to the imaging sessions, as it has been shown in previously published work that fasting of mice prior to PET imaging studies greatly improved visualization of tumor xenografts [23]. PET imaging was performed using 2% isoflurane anesthesia in oxygen at 0.8 L/min. The lateral tail veins of the mice were catheterized and injected with 3.23 ±2.48 MBq of [^{68}Ga]-DOTA-en-pba in a volume of 210 ± 10 μL. Three different dynamic PET acquisitions were performed for 60 min post injection. During the scans, body temperature of the animals was maintained at 36 °C on the scanner bed. PET scans were performed using a Mediso scanner (Mediso NanoScan PC, with 8 detector modules) with an axial field of view of 98.6 mm and a spatial resolution of 0.8 mm at the center of the scanner (with Tera-Tomo 3D PET iterative reconstruction). After PET imaging, a CT scan was obtained for attenuation correction and anatomic localization. The X-ray beam energy set at 50 kVp, the exposure time at 300msec and current at 670 μA. The number of projections per rotation was 480 and the slice thickness 250 μm. For the CT

image reconstruction, a modified version of the Feldkamp algorithm and the Ram-Lak filter were used. PET and CT data were reconstructed using Nucline software version 2.01 (Build 011.0005). The PET list-mode data were reconstructed into 26 frames (12 × 10 s, 3 × 60 s, and 11 × 300 s) using a version of 3D OSEM algorithm (Tera-Tomo 3D PET image reconstruction algorithm). The voxels dimension of PET and CT images were 0.4 x 0.4 x 0.4 mm and 0.25 × 0.25 × 0.25 mm respectively. Dead time, decay, scatter, attenuation and axial sensitivity corrections as well as normalization were applied to PET data. Image analysis was performed with the software InterView Fusion 3.00.039.0000 BETA.

Statistical analysis

The data are presented as means ± standard deviations. For the biodistribution studies, the data were compared using an unpaired t-test with a significance level of $P < 0.05$. All analyses were performed using Microsoft Office Excel.

Results

Preparation and stability assessment of [^{68}Ga]-DOTA-en-pba

The DOTA-en-pba chelate was prepared following the procedure reported previously [14] and efficiently labeled with gallium-68 by heating the solution for 30 min at 90 ºC, resulting in high radiochemical yield (≥ 98%) and purity (≥ 98%) of the complex (Rf = 9 min) as determined by HPLC (Fig. 1a,b and S1). When 80 MBq ^{68}Ga was used for the radiolabeling, the specific activity of the radiolabeled product was 661.2 MBq/μmol at the end of synthesis. Stability of the radiolabeled complex was evaluated up to 3h - the maximum time allowed by the half-life of gallium-68. The complex, incubated in saline at room temperature and in human serum at 37 ºC, was demonstrated to be intact in both media during the assessment time (Table 1).

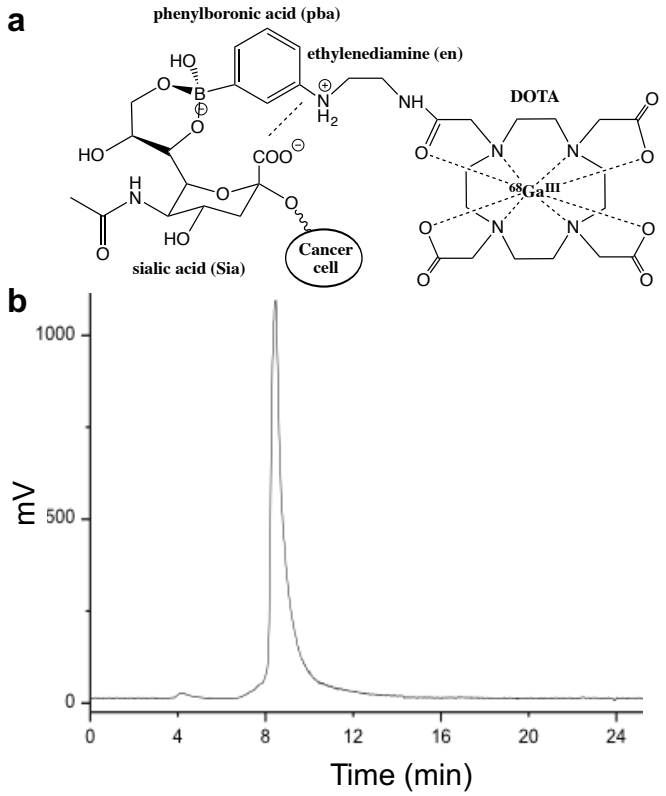

Fig. 1 PET radiotracer [^{68}Ga]-DOTA-en-pba: **a** Chemical structure of the complex with indication of functionalities: DOTA = complexation, en = linker, positively charged at physiological pH, participates with the cooperative binding with the negatively charged cell surface, pba = targeting vector, recognizes Sia on the cell surface through the binding with diol function. **b** HPLC chromatogram representing radiochemical purity.

Table 1 Results on stability assessment of [^{68}Ga]-DOTA-en-pba in saline and human serum.

Cell line	Cell uptake w/o block (%)	Cell uptake w/ block (%)	Melanin Absorption (490 nm)	Sia (nmol/mg protein)
B16-F10	21	4	2.5 ± 0.4	7.3 ± 0.6
Mel-C	11	3	0.6 ± 0.1	2.0 ± 0.7

In vitro binding studies

The cell binding assays were performed on human (Mel-C) and mouse (B16-F10) melanoma cell lines by incubation with [^{68}Ga]-DOTA-en-pba for 1h. The cell uptake by Mel-C and B16-F10 cells was found to be ~3.5 and ~5 times higher, respectively, compared to the uptake after

blocking the cells with an excess unlabeled DOTA-en-pba (Table 2). These results are in perfect agreement with the differences in melanin production determined by its absorbance measured on cell lysates at 490 nm, as well as Sia-expression measured using a Sia assay (abCAM). Both melanin production and Sia-expression are 4 times higher in B16-F10 with respect to Mel-C. Based on these results, B16-F10 cells were used as an *in vivo* model to demonstrate the capability of [^{68}Ga]-DOTA-en-pba to report on Sia-expression.

Table 2 Comparison of two melanoma cell lines concerning production of melanin, overexpression of Sia, and cell uptake after incubation with [^{68}Ga]-DOTA-en-pba without (w/o) and with (w/) blockage by the unlabeled precursor.

	Saline	**Human Serum**
30 min	> 98%	> 95%
60 min	≥ 98%	≥ 95%
180 min	≥ 98%	≥ 95%

Biodistribution studies of [^{68}Ga]-DOTA-en-pba

Biodistribution studies with [^{68}Ga]-DOTA-en-pba were conducted in B16-F10 and Mel-C tumor-bearing SCID mice at 20, 40 and 120 min p.i. (Fig. 2 and Table S1). Biodistribution studies in Mel-C tumor-bearing SCID mice showed no significant blood clearance at the time points studied. The excretion route was primarily via the urinary tract, as no significant liver and intestinal uptake was observed. Apart from the kidneys, no major uptake in all analyzed tissues was observed (≤ 2% ID/g from 30 min p.i.). Uptake in the tumor peaked at 30 min p.i. (2.07% ID/g ± 0.47%) and decreased after 1 h p.i. (1.23% ± 0.40% ID/g). The tumor-to-blood ratio remained below 1 at all time-points studied, suggesting a low tumor-to-background ratio.

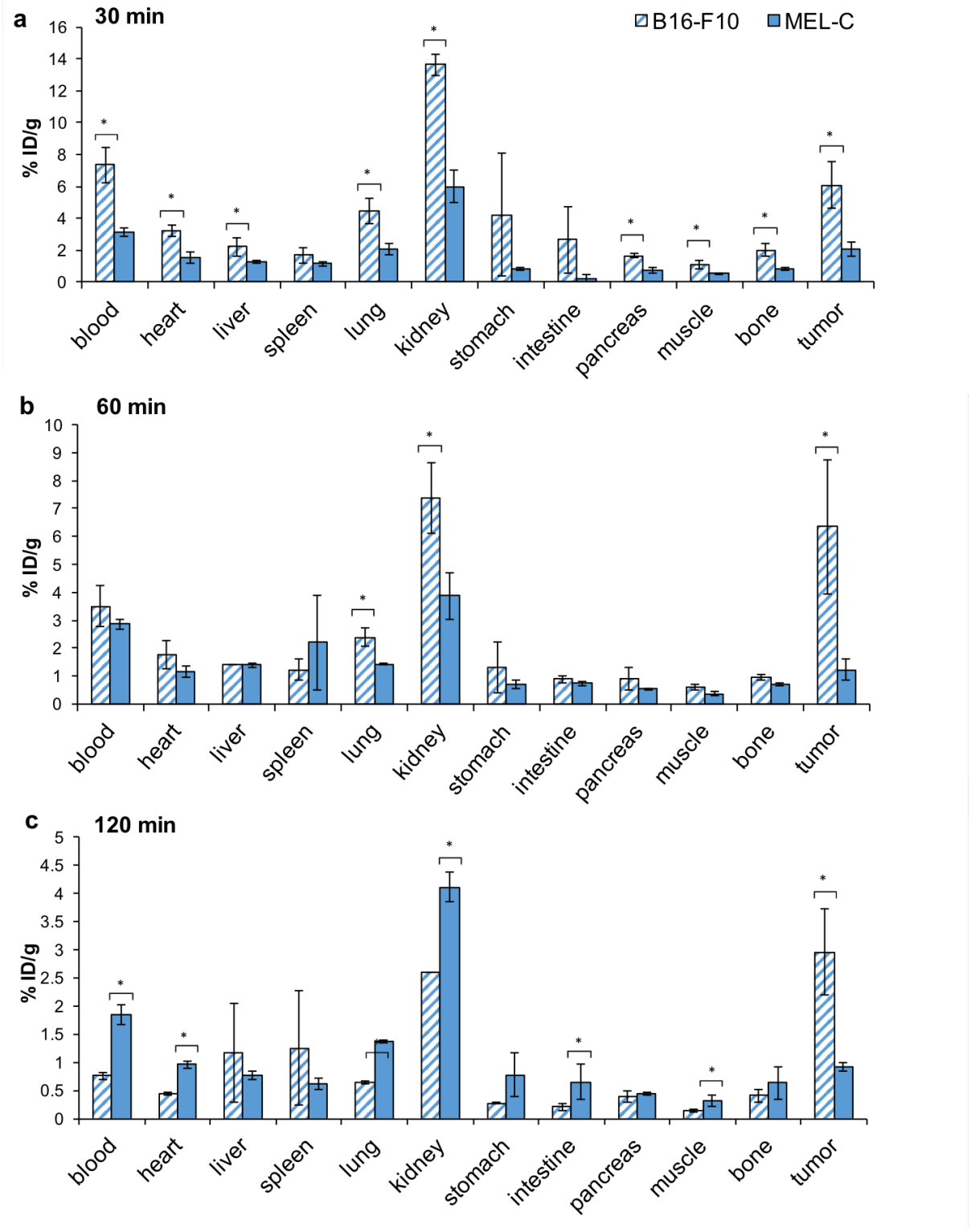

Fig. 2 Biodistribution studies of [^{68}Ga]-DOTA-en-pba in B16-F10 and Mel-C melanoma tumor-bearing SCID mice at **a** 30, **b** 60, and **c** 120 min post-injection. Mean (%ID/g) ± SD at each time-point (n = four animals per time-point); significant differences ($P < 0.05$) are denoted with an asterisk. The full data set is given in Table S1.

At the same time, the tumor-to-muscle ratio reached 3.76 at 30 min p.i., suggesting a clear differentiation between the affected and the non-affected tissues (Fig. 3).

In the case of the B16-F10 tumor model, the radiotracer was rapidly cleared from blood (% ID/g: 7.35 ± 1.14, 3.49 ± 0.73, 0.76 ± 0.06 at 30, 60 and 120 min p.i.). Fast clearance was also observed from the heart, lungs and muscle. High percentage of radioactivity in kidney, in combination with low uptake in the liver and intestines, indicate that the predominant route of excretion is the urinary system. It is important to note that tumor uptake of the radiotracer accumulated very quickly, and was clearly visible at 30 min p.i. (6.06 ± 1.45 %ID/g), showing a slight increase at 60 min p.i. (6.36 ± 2.41 %ID/g) and then decreasing at 120 min p.i. (2.96 ± 0.77% ID/g). At all time-points studied, tumor uptake was significantly different ($P < 0.05$) between the two different tumor models, in favor of the B16-F10 tumor model. Even though there is a decrease in tumor uptake at 120 min p.i., the tumor-to-blood ratio increased from 60 to 120 min (1.79 ± 2.41% and 3.94 ± 1.31%, respectively), which is also the case for tumor-to-muscle ratios (10.77 ± 2.31 and 20.21 ± 2.36 at 60 and 120 min, respectively) (Fig.3).

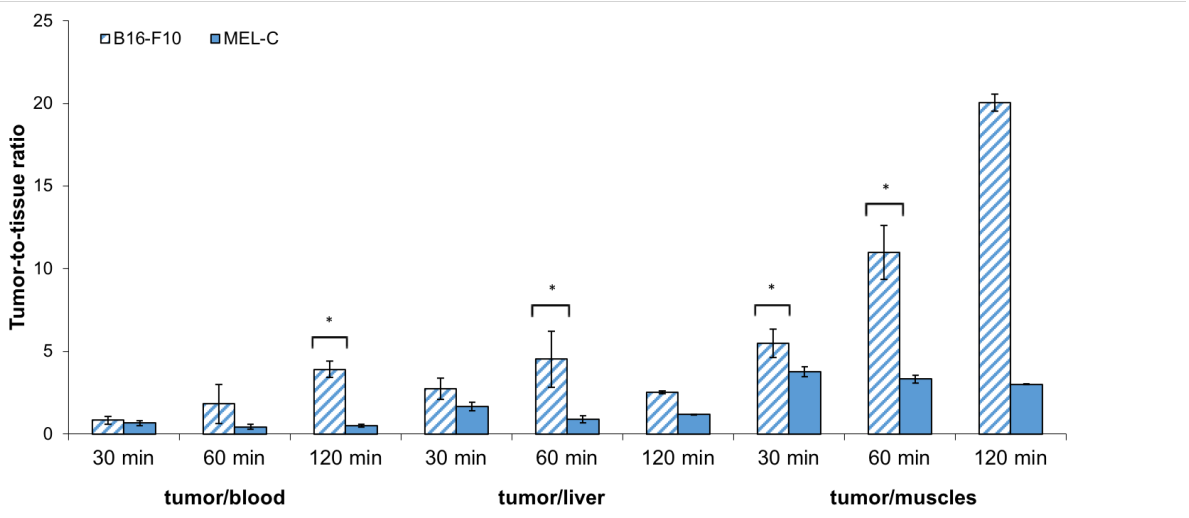

Fig. 3 Tumor-to-tissue ratios in B16-F10 and Mel-C tumor-bearing SCID mice at 30, 60 and 120 min post-injection. Significant differences ($P < 0.05$) are denoted with an asterisk.

The specificity of the pba targeting to B16-F10 tumor *in vivo* has already been demonstrated by MRI using paramagnetic Gd^{III}-DOTA-en-pba [14]. In this competition study, the mice were pre-injected with a diamagnetic Lu^{III}-analogue and 60% decrease in accumulation of the post-injected contrast agent in tumor was observed. In the current study, binding specificity of [^{68}Ga]-DOTA-en-pba was investigated by performing blocking experiments in B16-F10 melanoma tumor-bearing mice at 60 min post-injection of the radiotracer, after pre-injection of the mice with a 50 x excess (i.e.0.2875 μmol) unlabeled DOTA-en-pba. Blood, tumor and liver uptake were significantly different ($P < 0.05$) between the blocked and unblocked mice (Fig.S4) (~75% accumulation decrease in the B16-F10 tumor), thus confirming the binding specificity of [^{68}Ga]-DOTA-en-pba.

Metabolite studies

Metabolite studies were performed on tumor, blood and urine samples taken from B16-F10 tumor-bearing SCID mice injected with [^{68}Ga]-DOTA-en-pba. A single peak corresponding to [^{68}Ga]-DOTA-en-pba was observed from the tumor sample (Fig. S2), with no other radioactive components present, suggesting that the radioactivity in the tumor is entirely attributable to non-metabolized [^{68}Ga]-DOTA-en-pba. Similar results were obtained for blood and urine samples (Fig. S3).

Imaging studies

In light of the above biodistribution results, we proceeded with *in vivo* PET imaging of the B16-F10 melanoma tumor model. Figure 4 shows PET images of one of the B16-F10 tumor-bearing mouse at different time points after injection of [^{68}Ga]-DOTA-en-pba. The images demonstrate localization of the radiotracer at the tumor, and a clear delineation of the tumor up to 60 min p.i. Volumes of interest (VOIs) for tumor and muscle of the same size for each image

were drawn, and showed that tumor-to-muscle ratios from the PET study were in agreement with the results of the biodistribution study (Table S2 and Fig. S5).

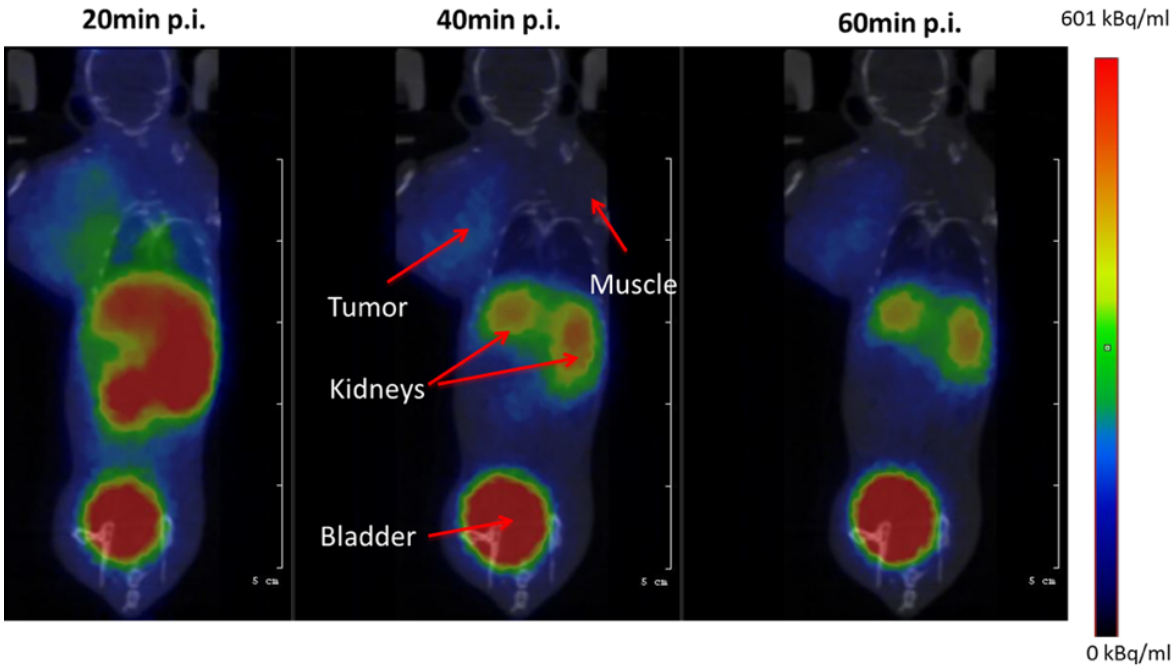

Fig. 4 *In vivo* PET imaging of [^{68}Ga]-DOTA-en-pba on SCID mice bearing B16-F10 melanoma tumor, showing a clear delineation of the tumor from 20 min p.i.

Discussion

Early disease detection can make an immense difference in the final outcome of a patient with cancer. The identification of tumor targets for the development of appropriate imaging probes has been and still is an ongoing challenge. The interaction of a biomarker with a specific extracellular agent should lead to satisfactory delivery of the imaging probe. Thus, for imaging purposes, targeting efficiency mainly relies on the overexpression of the targeted moiety on the cell surface. It is well known that Sia is overexpressed on the surface of cancerous cells as a terminal group on the oligosaccharide chains of glycolipids and glycoproteins [24]. Numerous studies have shown that sialic acid, which has a 1000× higher expression on tumor cells

compared to normal cells, can be considered as a promising biomarker for cancer recognition and determination of metastatic activity of tumors [25]. Furthermore, the amount of Sia expression on cancer cells correlates with patient prognosis [26-27].

In our previous work, we designed a Gd^{III}-DOTA-based MRI CA, conjugated with a phenylboronic targeting vector through an ehylenediamine linker [14]. The latter functionality, being positively charged at physiological pH, was shown to facilitate the binding by electrostatic interaction with the negatively charged cell surface [28], while the targeting occurred due to the formation of 5- and 6-membered ring boronate esters with the diol function of Sia (Fig. 1a). The specificity of this binding *in vivo* was demonstrated earlier by the injection of diamagnetic Lu^{III}-labeled analogue into a melanoma tumor bearing mice, prior to administration of the Gd^{III}-DOTA-en-pba, which resulted in no p.i. contrast. In comparison, a bright contrast was observed due to accumulation of the paramagnetic CA at the tumor site [14]. The association binding constant (K_D) of 270 μM determined by measuring the longitudinal relaxation rates ($R_{1,}$ s^{-1}) of B16-F10 cells (sia expression = 7.3×10^{-9} mol/mg proteins) after incubation with Gd^{III}-DOTA-en-pba is in a perfect agreement with the values typical for targeting contrast agents [29].

With the current study, we extend the application of the designed targeting compound to the *in vivo* detection of Sia by a more sensitive radionuclide imaging technique such as PET. After efficient radiolabeling of the chelate with gallium-68 with > 98% radiochemical purity, the targeting capability of [^{68}Ga]-DOTA-en-pba to the Sia-residue on the tumor cells was demonstrated *in vitro* on the Mel-C and B16-F10 melanoma cells. Melanin production and Sia-expression were also evaluated in both cell lines, to demonstrate Sia overexpression, which is directly correlated to melanogenesis. These *in vitro* studies showed that [^{68}Ga]-DOTA-en-pba had a more pronounced affinity on B16-F10 melanoma cells and that both melanin and Sia production are 3-4 times higher, compared to Mel-C melanoma cells. The results from the *ex*

vivo biodistribution study on the B16-F10 tumor model show a more pronounced differentiation between the affected and non-affected tissue, with respect to the results of the Mel-C tumor model. The significant increase in tumor/blood and tumor/muscle ratios observed in B16-F10 tumor mice model compared to the Mel-C tumor model confirms the obtained *in vitro* results, i.e. [^{68}Ga]-DOTA-en-pba is also a specific *in vivo* reporter of Sia-expression, exhibiting *in vivo* behavior relevant to melanin production and Sia overexpression. Blocking studies performed on the B16-F10 melanoma tumor model proved binding specificity of the radiotracer. The acquired PET images were in accordance to the *ex vivo* biodistribution results, as shown for the B16-F10 tumor model.

For effective translation of a radiolabeled imaging agent to the clinics, it is very important to evaluate the degree to which the association between the radiolabel and the core molecule remains intact *in vivo*. In our case, it is critical to assess the stability of DOTA-en-pba radiolabeled with gallium-68, once administered into systemic circulation. Therefore, one of the objectives of this work was to study the *in vivo* integrity of [^{68}Ga]-DOTA-en-pba. One of the most important findings of the present work is that the radioactivity in the tumor samples is entirely attributable to the intact radiotracer [^{68}Ga]-DOTA-en-pba, as is the case for blood and urine samples.

Conclusions

We have successfully prepared and tested a radiolabeled form of DOTA-derivative functionalized with phenylboronic targeting vector for tumor detection with PET imaging. High concentrations of [^{68}Ga]-DOTA-en-pba have been detected at tumor sites after intravenous injection, confirming high specificity of the tracer towards overexpressed sialic acid. We envision that this type of PET imaging agent can be combined with its MRI analogue, which has already been proved effective for tumor targeting. Such a combination can lead to improved diagnostic performance for cancer detection and estimate the metastatic potential of

various tumor types. As a result, Gd/^{68}Ga-DOTA-en-pba exhibits great potential for PET/MR image-guided therapy of cancer. We are currently working on the assessment of [^{68}Ga]-DOTA-en-pba in other tumor types overexpressing sialic acid.

Acknowledgements. The authors gratefully acknowledge Mr. S. Xanthopoulos (Radiochemical Studies Laboratory, INRaSTES, NCSR "Demokritos") and Mr. E. Balafas (Laboratory Animal Facilities, Biomedical Research Foundation of the Academy of Athens) for excellent technical assistance.

Compliance with Ethical Standards

Conflict of interest

The authors declare that they have no conflict of interest.

References

1. Henry NL, Hayes DF (2012) Cancer biomarkers. Mol Oncol 6:140-146.
2. Mankoff DA, Pryma Da Fau - Clark AS, Clark AS (2014) Molecular imaging biomarkers for oncology clinical trials. J Nucl Med 55:525-528.
3. de Jong M (2017) New tracers to the clinic. Q J Nucl Med Mol Imaging 61:133-134.
4. Bernsen MR, Kooiman K, Segbers M, van Leeuwen FWB, de Jong M (2015) Biomarkers in preclinical cancer imaging. Eur J Nucl Med Mol Imaging 42:579-596.
5. Fani M, Maecke HR (2012) Radiopharmaceutical development of radiolabelled peptides. Eur J Nucl Med Mol Imaging 39 Suppl 1:S11-30.
6. Pinho SS, Reis CA (2015) Glycosylation in cancer: mechanisms and clinical implications. Nat Rev Cancer 15:540-555.
7. Pearce OM, Laubli H (2016) Sialic acids in cancer biology and immunity. Glycobiology 26:111-128.

8. Tanaka F, Otake Y, Nakagawa T, et al. (2001) Prognostic Significance of Polysialic Acid Expression in Resected Non-Small Cell Lung Cancer. Cancer Res 61:1666.

9. Falconer RA, Errington RJ, Shnyder SD, Smith PJ, Patterson LH (2012) Polysialyltransferase: a new target in metastatic cancer. Curr Cancer Drug Targets 12:925-939.

10. Julien S, Bobowski M, Steenackers A, Le Bourhis X, Delannoy P (2013) How Do Gangliosides Regulate RTKs Signaling? Cells 2:751-767.

11. Büll C, Boltje TJ, van Dinther EAW, et al. (2015) Targeted Delivery of a Sialic Acid-Blocking Glycomimetic to Cancer Cells Inhibits Metastatic Spread. ACS Nano 9:733-745.

12. Uemura T, Shiozaki K, Yamaguchi K, Miyazaki S, et al. Contribution of sialidase NEU1 to suppression of metastasis of human colon cancer cells through desialylation of integrin beta4. Oncogene 28:1218-1229.

13. Kimoto M, Ando K, Koike S, et al. (1993) Significance of platelets in an antimetastatic activity of bacterial lipopolysaccharide. Clin Exp Metastasis 11:285-292.

14. Crich SG, Alberti D, Szabo I, Aime S, Djanashvili K (2013) MRI Visualization of Melanoma Cells by Targeting Overexpressed Sialic Acid with a GdIII-dota-en-pba Imaging Reporter. Angew Chem Int Ed 52:1161-1164.

15. Blamire A M (2008) The technology of MRI: the next 10 years?. Br J Radiol 81: 601–617.

16. Kunjachan S, Jayapaul J, Mertens M E, Storm G, Kiessling F, Lammers T (2012) Theranostic Systems and Strategies for Monitoring Nanomedicine-Mediated Drug Targeting. Curr Pharm Biotechnol 13:609–622.

17. Toy R, Bauer L, Hoimes C, Ghaghada K, Karathanasis E (2014) Targeted Nanotechnology for Cancer Imaging. Adv Drug Deliv Rev 30:79–97.

18. Fani M, Andre JP, Maecke HR (2008) ^{68}Ga-PET: a powerful generator- based alternative to cyclotron-based PET radiopharmaceuticals. Contrast Media Mol Imaging 3:67-77.

19. Al-Nahhas A, Fanti S (2012) Radiolabelled peptides in diagnosis and therapy: an introduction. Eur Jo Nucl Med Mol Imaging 39:1-3.

20. Decristoforo C, Pickett RD, Verbruggen A (2012) Feasibility and availability of ^{68}Ga-labelled peptides. Eur J Nucl Med Mol Imaging 39:31-40.

21. Rosch F, Baum RP (2011) Generator-based PET radiopharmaceuticals for molecular imaging of tumours: on the way to THERANOSTICS. Dalton Trans 40:6104-6111.

22. Zhernosekov KP, Filosofov D, Baum RP, Aschoff P, et al. (2007) Processing of generator-produced ^{68}Ga for medical application. J Nucl Med 48:1741-1748.

23. Fueger BJ, Czernin J, Hildebrandt I, Tran C, Halpern BS, Stout D, Phelps ME, Weber WA. (2006) Impact of animal handling on the results of 18F-FDG PET studies in mice. J Nucl Med 47(6): 999-1006.

24. Schauer R (2000) Achievements and challenges of sialic acid research. Glycoconj J 17:485-499.

25. Martinez-Duncker I, Salinas-Marin R, Martinez-Duncker C (2011) Towards In Vivo Imaging of Cancer Sialylation. Int J Mol Imaging vol. 2011:1-10.

26. Cazet A, Julien S, Bobowski M, et al. (2010) Consequences of the expression of sialylated antigens in breast cancer. Carbohyd Res 345:1377-1383.

27. Fernandez-Briera A, Garcia-Parceiro I, Cuevas E, Gil-Martin E (2010) Effect of human colorectal carcinogenesis on the neural cell adhesion molecule expression and polysialylation. Oncology 78:196-204.

28. Djanashvili K, Koning GA, van der Meer AJGM, Wolterbeek HT, Peters JA (2007) Phenylboronate Tb-160 complexes for molecular recognition of glycoproteins expressed on tumor cells. Contrast Media Mol Imaging 2:35-41.

29. Caravan P, Zhang Z (2013) Targeted MRI Contrast Agents. In The Chemistry of Contrast Agents in Medical Magnetic Resonance Imaging. John Wiley & Sons, Ltd, pp 311-342.